# Infrared single-photon sensitivity in atomic layer deposited superconducting nanowires

(ID) **Gregor G. Taylor,** (ID) **Dmitry V. Morozov,** (ID) **Ciaran T. Lennon, et al.**

## COLLECTIONS

Paper published as part of the special topic on  Non-Classical Light Emitters and Single-Photon Detectors

View Online          Export Citation          CrossMark

---

### ARTICLES YOU MAY BE INTERESTED IN

AIP Publishing

# Infrared single-photon sensitivity in atomic layer deposited superconducting nanowires

View Online  Export Citation  CrossMark

Gregor G. Taylor,[1,a)] (iD) Dmitry V. Morozov,[1] (iD) Ciaran T. Lennon,[1] (iD) Peter S. Barry,[2] Calder Sheagren,[3] (iD) and Robert H. Hadfield[1] (iD)

## AFFILIATIONS

[1]James Watt School of Engineering, University of Glasgow, University Avenue, Glasgow G12 8QQ, United Kingdom
[2]Division of High Energy Physics, Argonne National Laboratory, Lemont, Illinois 60439, USA
[3]Kavli Institute for Cosmological Physics, University of Chicago, Chicago, Illinois 60637, USA

**Note:** This paper is part of the APL Special Collection on Non-Classical Light Emitters and Single-Photon Detectors.
[a)]Author to whom correspondence should be addressed: g.taylor.3@research.gla.ac.uk

## ABSTRACT

We report on the extended infrared single-photon response of niobium nitride superconducting nanowires deposited by atomic layer deposition. The superconducting nanowire single-photon detectors are based on 4.65 nm thick NbN, patterned into 100 nm meanders, and characterized at 2.5 K. We verify single-photon sensitivity from 1310 to 2006 nm with saturated response at shorter wavelengths.

Superconducting nanowire single-photon detectors (SNSPDs)[1] have matured in the last decade to become the lead choice for single-photon experiments due to their ultra-low dark count rates,[2] near-unity quantum efficiency,[3] long wavelength sensitivity,[4] and fast temporal resolution.[5] These characteristics have allowed their deployment into a diverse range of experimental demonstrations, including single-photon remote sensing[6] and life science applications.[7] In particular, their long wavelength sensitivity has recently been exploited to enable photon pair sources[8] and single-photon LIDAR[9] in the mid-infrared region, beyond the reach of conventional photon counting technologies. Material development plays a key role in SNSPD fabrication as the superconducting energy gap and critical temperature ($T_c$) varies between materials[10] and influences the detection characteristics and cooling requirements. Recent work has also indicated that reducing material inhomogeneities will allow operation at a larger fraction of the depairing current[11] as well as being desirable for fabrication of large-area SNSPDs.[12]

Atomic layer deposition (ALD) is a subclass of chemical vapor deposition (CVD) based on the sequential, self-limiting exposure of individual gas-phase precursor species, forming a single atomic layer of material. A single deposition step, known as an "ALD cycle," can then be repeated *ad infinitum* to form a film of desired thickness with Ångstrom-level sensitivity.[13] In the specific case of plasma-enhanced ALD (PEALD), an additional plasma exposure step is added after precursor exposure to remove unreacted material by-products.[14] The self-limiting nature of the ALD process removes the statistical aspect of conventional deposition techniques (such as sputtering), where localized areas of the surface often react first due to the randomness of precursor flux, creating rough and pinhole-laden films. Consequently, ALD films are highly uniform and conformal as well as pinhole-free.[13,15,16] ALD translates well to large area deposition, with the only limit being the size of the deposition chamber as well as concurrent processing of multiple substrates. Recent developments in the use of ALD for deposition of high quality superconducting metal nitrides have consequently made it an attractive technique for the fabrication of superconducting technologies, with particular progress in the use of PEALD for the deposition of NbN and TiN thin films, respectively.[17–19] These material advances, coupled with the unparalleled uniformity and conformality of ALD, therefore make this growth technique an ideal candidate for the fabrication of SNSPDs.

To date, the large majority of NbN SNSPDs have been fabricated using thin films grown via reactive sputtering.[20] A large study[21] of the film properties of ALD NbN was performed, and saturated photon counting was demonstrated in the near-IR. Other researchers have reported on large scale depositions[22] of ALD NbN SNSPDs and verified the uniformity of devices based on this technique. In this work, we fabricate SNSPDs on ALD NbN and verify their candidacy for single-photon detection in the 1310 to 2006 nm infrared spectral range.

ALD films were grown at the University of Chicago with organic based precursors. Films were deposited on high resistivity Si ⟨100⟩ substrates with resistivity of >10 k Ω·cm, which were cleaned with organic solvents before deposition. We then let the chamber and substrate temperature stabilize in vacuum for an hour before starting the process. We used TBTDEN precursor and $N_2/H_2$ plasma in each deposition cycle, while the substrate was heated to 300 °C. In our initial optimization of the ALD NbN deposition process, we targeted a NbN thickness similar to that used by many leading groups employing reactive sputtered NbN for SNSPDs[23] and aimed for a film thickness of 4.65 nm with 75 ALD cycles at approximate rate of 0.6 Å per cycle.[19]

We then fabricated SNSPDs at the James Watt Nanofabrication Center (Glasgow) with 100 kV electron-beam lithography and plasma etch. First, Ti/Au alignment markers and contact pads were formed with a loft-off procedure. We then used ZEP520 as an etch mask and $SF_6/N_2$ plasma to etch the meander structure. The SNSPD meander covers an active area of $10 \times 9.6 \ \mu m^2$ and has a linewidth of 100 nm with a fill factor of 0.5. A scanning electron microscope image of a nanowire is shown in Fig. 1(a). Transmission electron microscopy (TEM) was carried out in the Kelvin Nanocharacterisation Center (University of Glasgow) using a FEI Technai T20 microscope. Samples were prepared using a conventional focused ion beam lift-out technique.[24] The TEM samples were prepared from a 200 nm width nanowire meander device from the same fabrication run and film as the 100 nm width device optically tested below. Images are shown in Fig. 1(b). From the TEM images, we estimate the NbN film thickness to be 4.529 nm with a 1.57 nm native oxide layer on top.

For this fabrication run, four detectors of identical geometries (100 nm width) were fabricated. The switching current, $I_{sw}$, was determined for each tested device by slowly increasing the bias current to a shielded detector until the output pulse count dropped to zero. For the device presented here, the $I_{sw}$ values was 5.16 $\mu$A at 2.5 K. We then fiber coupled this device for optical testing.

The SNSPD was coupled with Corning SMF-28 optical fiber and cooled to an operating temperature of 2.5 K in a Gifford-McMahon closed-cycle cryocooler. Electrical pulses were readout using a cryogenic amplifier (Cosmic Microwave Technology CITLF1) mounted on the 40 K stage which also housed a bias-tee to current bias the detector. Near IR illumination was provided by a set of CW laser diodes at wavelengths of 1310 and 1550 nm which were sent through a pair of programable optical attenuators to attenuate the input to single-photon levels. The methodology follows the calibrated single-photon detection procedure detailed previously.[25] The photon flux rate was set by measuring the optical power at the input of the cryostat and then applying appropriate attenuation with the programable attenuators. This attenuated output was then connected to the fiber coupled to the detector. For the 2006 nm measurements, the source was an optical parametric oscillator (OPO, Chromacity Ltd) tunable from 1.5 to 4.2 $\mu$m. This provided short, ps, pulses at 110 MHz. The output was filtered with a 2006 nm narrow bandpass filter and then attenuated by chaining four MEMS-based variable optical attenuators (VOAs). Each of the four VOAs was calibrated individually using an extended InGaAs power meter. The power was measured at both the input and output of each attenuator and then by adjusting the voltage to VOA the attenuation was set. By measuring the input power to the VOA setup and individually calibrating each VOA before chaining them all
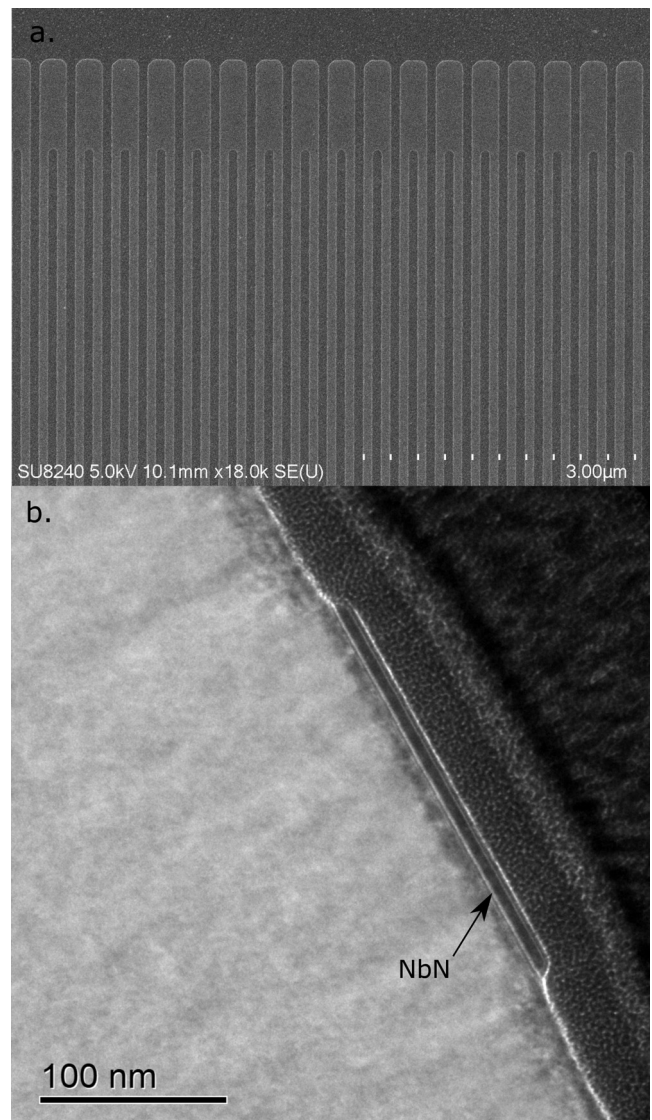


**FIG. 1.** (a) SEM image of fabricated nanowire of 100 nm width, identical to the device used for optical testing. (b) TEM cross section of 200 nm wide nanowire from same fabrication run and film as the optically tested device. Si substrate is shown in light gray. The material observed in the right of the image on top of the nanowire is Pt deposited during the TEM sample preparation process.
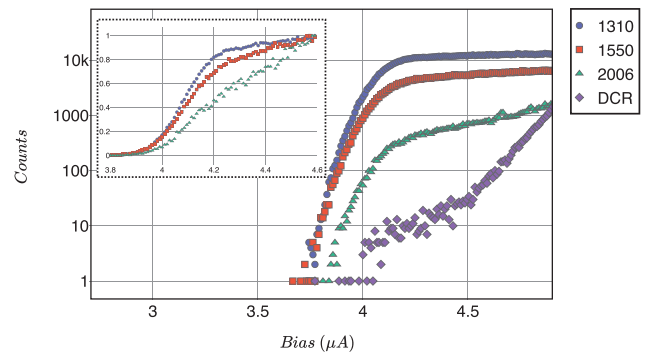
together, the photon flux was set to the desired rate. For all wavelengths measured, the photon flux was set to 1 MHz. A diagram of the setup is shown in Fig. 2(a). An example output pulse is shown in Fig. 2(b). The reflections present in the pulse shape are an artifact of the cryogenic amplifier used and were not present if a different set of room-temperature amplifiers was used. From the pulse, we can determine the rise time to be 1.4 ns and by fitting the decaying pulse with an exponential function we calculate the 1/e decay time to be 32 ns. From this, we can estimate the maximum count rate of the device to be around 30 MHz. The superconducting transition temperature, $T_c$, of the device was measured using a resistor heater located on the 2.5 K
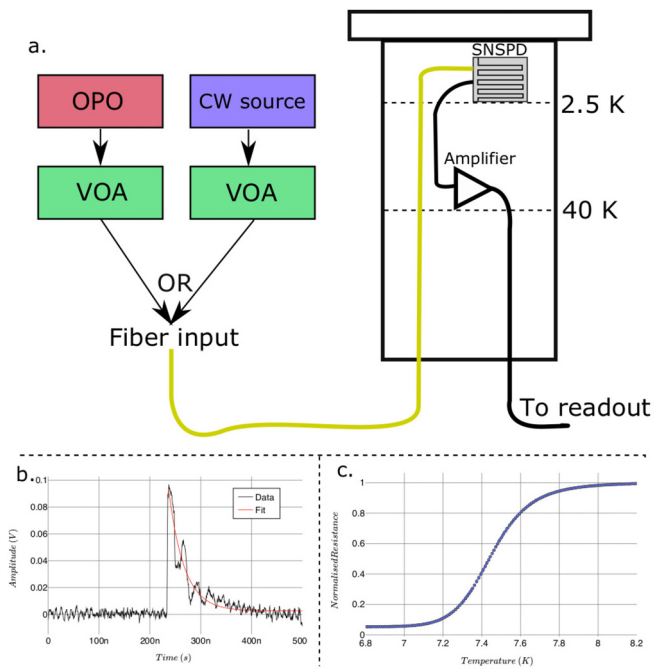
**FIG. 2.** (a) Experimental setup. The light source is either an OPO for the mid-IR (2006 nm) or a CW laser diode for the near-IR (1310, 1550 nm). Light is attenuated in the variable optical attenuators (VOA) and calibrated at the fiber input. Output pulses from the SNSPD are amplified and sent out to the readout. (b) Example of an output pulse from the SNSPD. The reflections are an artifact of the cryogenic amplifier used and the decay time calculated from the exponential fitting (red) is 32 ns. (c) Resistance–temperature plot for SNSPD presented. The $T_c$ is 7.4 K at the mid-point of the transition.



**FIG. 3.** PCR curves for wavelengths of 1310, 1550, and 2006 nm. The dark count rate (DCR) is also shown. Inset: Same plots on a linear scale with the maximum photon counts normalized for each wavelength.

stage of the cryostat to slowly heat up and cooldown the detector, recording the resistance in a two-point measurement. The R–T plot is shown in Fig. 2(c). We take the $T_c$ as the point where the resistance has dropped to half of its normal-state value and determine this to be 7.44 K. The transition width is determined between the points where the resistance is 90% and 10% of its normal-state value and we observe a transition width of 0.52 K.

The photon count rate (PCR) curves were taken by varying the bias current up to the $I_{sw}$ while the pulses from the SNSPD were counted using a universal counter (Agilent 53131A). The detection threshold on the counter was set to 70% of the pulse height to avoid false counts caused by the reflections in the output pulse. The results are shown for wavelengths of 1310, 1550, and 2006 nm in Fig. 3. The saturation of internal detection efficiency manifests itself as a plateau in the PCR curve, indicating that efficiency no longer increases with increasing bias current. For wavelengths of 1310 and 1550 nm, evidence of a saturated plateau is observed, whereas for 2006 nm the efficiency continues to climb with increasing bias current. The inset of Fig. 3 shows the same data, normalized to one for each wavelength and plotted on a linear scale for clarity. For the PCR curves, the dark counts have been subtracted from the photon counts to account for the background photon flux. The dark count rate for the device is also shown in Fig. 3. It is noted in the PCR curves that the PCR continues to climb past the saturated region when bias is increased, particularly

for the 2006 nm measurement. It is hypothesized that this is caused by a non-uniform switching current along the length of the nanowire, either caused by fabrication imperfections or current crowding effects in the bends of the meander.[26] This causes a saturation of the detection efficiency for the majority of the nanowire while there remains spots of higher $I_{sw}$ that continue to increase in detection efficiency as the bias is further increased. However, the presence of the inflection point in the PCR curves,[27] evident at all wavelengths, is indication we are operating above the cutoff current, $I_{co}$. Above $I_{co}$ the device is operating in the single-photon detection regime,[28] not in the probabilistic regime for each wavelength.

The timing jitter of an SNSPD is an important metric for time-of-flight photon counting experiments,[29] fiber optic sensing,[30] quantum key distribution,[31] and deep space optical communications[32] where it enhances the ability to determine weak signals in the presence of background noise. To measure the timing jitter, $\Delta t$, we utilized a pulsed fiber laser at 1550 nm giving fs pulses at 50 MHz. We split the output with a 90:10 optical splitter and sent a portion to a photodetector to act as a sync signal for a Becker and Hickl time correlated single-photon counting card (SPC-150-NXX). The other portion of the split optical signal was attenuated to single-photon levels and sent to the detector as per the PCR curve experiments. By integrating, we obtained a timing histogram of the variation of SNSPD pulse arrival times with respect to the sync signal. The full-width-half-maximum (FWHM) value of this is defined as $\Delta t$. Figure 4 shows a $\Delta t$ of 50.4 ps for the 1550 nm jitter test. For this test, the detector was biased at 0.93 $I_{sw}$.

In this work, we have demonstrated the single-photon sensitivity of ALD NbN nanowires to infrared light up to a wavelength of 2006 nm. We have measured the timing jitter and single-photon response and found it to be comparable to results for similar sputtered devices. The photon responses presented here are for bare superconducting nanowires, that is, a nanowire with no optical absorption enhancement. Embedding the nanowire into an optical cavity to enhance absorption at specific wavelengths[33,34] would enhance the photon response greatly as per previously published work. It is also worth noting that for the 2006 nm measurement, we are operating outside of the specified wavelength regime for SMF-28 fiber, and therefore, additional loss in the cryostat will be encountered. This will manifest itself as a reduction in the overall detection efficiency at longer wavelengths. Future work will include coupling with specialist
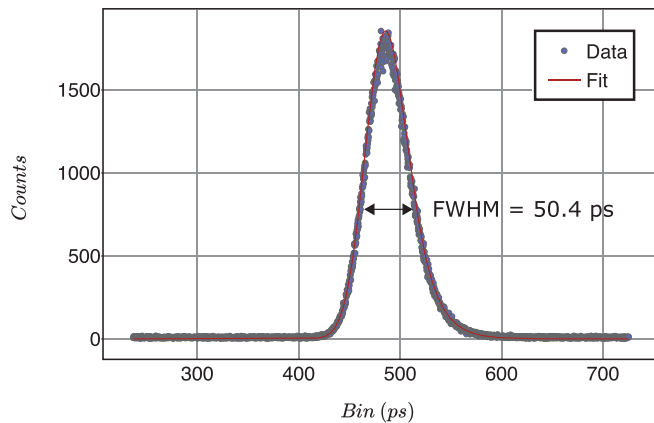
**FIG. 4.** Timing jitter histogram for ALD device at 1550 nm. The data have been fitted with an exponentially modified Gaussian function to determine the FWHM value.

mid-infrared fiber to combat this issue. The timing jitter is for a meander type device where no steps have been taken to mitigate the geometric component of the timing jitter associated with the meandering wire.[35] The evidence of saturated internal efficiency is a good indicator of the quality of the ALD film and shows the promise of this technology for SNSPDs. The next steps are to deposit NbN via ALD in an optical cavity type structure designed for use in the mid-infrared. Full optical characterization of ALD NbN thin films in order to compare it more fully to sputtered NbN[36] will also be performed. Optimizing film deposition is an ongoing area of enquiry with the goal to deposit thin films of consistently high uniformity from which constriction-free nanowires can be fabricated.

In conclusion, we have demonstrated extended infrared single-photon sensitivity in SNSPD fabricated with ALD NbN with large area ($10 \times 10\,\mu m^2$) meander SNSPDs that are suitable for fiber optic coupling. We have demonstrated operation in the saturated internal detection efficiency regime of this material for wavelengths up to 2006 nm. This demonstrates the viability of this growth technique, particularly for future work where reducing inhomogeneities in thin films in order to increase detector efficiency at long wavelengths will be the goal. This will also aid in the pursuit of scaling up devices to larger areas.[37] The next stage is to produce ALD NbN SNSPDs integrated in optical cavities for the mid-infrared to better investigate their detection characteristics at such wavelengths and enhance the system detection efficiency. Further optimization of the ALD growth process in order to tune material composition and structure is also planned.

## DATA AVAILABILITY

The data supporting the findings of this study will be available via the University of Glasgow research data management online repository.

## REFERENCES

[1]G. Gol'tsman, O. Okunev, G. Chulkova, A. Lipatov, A. Semenov, K. Smirnov, B. Voronov, A. Dzardanov, C. Williams, and R. Sobolewski, "Picosecond superconducting single-photon optical detector," Appl. Phys. Lett. **79**, 705–707 (2001).

[2]H. Shibata, K. Shimizu, H. Takesue, and Y. Tokura, "Ultimate low system dark-count rate for superconducting nanowire single-photon detector," Opt. Lett. **40**, 3428–3431 (2015).

[3]D. V. Reddy, R. R. Nerem, S. W. Nam, R. P. Mirin, and V. B. Verma, "Superconducting nanowire single-photon detectors with 98% system detection efficiency at 1550 nm," Optica **7**, 1649–1653 (2020).

[4]V. Verma, B. Korzh, A. Walter, A. Lita, R. Briggs, M. Colangelo, Y. Zhai, E. Wollman, A. Beyer, J. Allmaras, B. Bumble, H. Vora, D. Zhu, E. Schmidt, K. Berggren, R. Mirin, S. Nam, and M. Shaw, "Single-photon detection in the mid-infrared up to 10 micron wavelength using tungsten silicide superconducting nanowire detectors," arXiv:2012.09979 (2020).

[5]B. Korzh, Q.-Y. Zhao, J. P. Allmaras, S. Frasca, T. M. Autry, E. A. Bersin, A. D. Beyer, R. M. Briggs, B. Bumble, M. Colangelo, G. M. Crouch, A. E. Dane, T. Gerrits, A. E. Lita, F. Marsili, G. Moody, C. Pena, E. Ramirez, J. D. Rezac, N. Sinclair, M. J. Stevens, A. E. Velasco, V. B. Verma, E. E. Wollman, S. Xie, D. Zhu, P. D. Hale, M. Spiropulu, K. L. Silverman, R. P. Mirin, S. W. Nam, A. G. Kozorezov, M. D. Shaw, and K. K. Berggren, "Demonstration of sub-3 ps temporal resolution with a superconducting nanowire single-photon detector," Nat. Photonics **14**, 250–256 (2020).

[6]A. McCarthy, N. J. Krichel, N. R. Gemmell, X. Ren, M. G. Tanner, S. N. Dorenbos, V. Zwiller, R. H. Hadfield, and G. S. Buller, "Kilometre-range, high resolution depth imaging via 1560 nm wavelength single-photon detection," Opt. Express **21**, 8904–8915 (2013).

[7]N. R. Gemmell, A. McCarthy, B. Liu, M. G. Tanner, S. D. Dorenbos, V. Zwiller, M. S. Patterson, G. S. Buller, B. C. Wilson, and R. H. Hadfield, "Singlet oxygen luminescence detection with a fiber-coupled superconducting nanowire single-photon detector," Opt. Express **21**, 5005–5013 (2013).

[8]S. Prabhakar, T. Shields, A. C. Dada, M. Ebrahim, G. G. Taylor, D. Morozov, K. Erotokritou, S. Miki, M. Yabuno, H. Terai, C. Gawith, M. Kues, L. Caspani, R. H. Hadfield, and M. Clerici, "Two-photon quantum interference and entanglement at 2.1 $\mu m$," Sci. Adv. **6**, eaay5195 (2020).

[9]G. G. Taylor, D. Morozov, N. R. Gemmell, K. Erotokritou, S. Miki, H. Terai, and R. H. Hadfield, "Photon counting LIDAR at 2.3 $\mu m$ wavelength with superconducting nanowires," Opt. Express **27**, 38147–38158 (2019).

[10]A. E. Lita, V. B. Verma, R. D. Horansky, J. M. Shainline, R. P. Mirin, and S. Nam, "Materials development for high efficiency superconducting nanowire single-photon detectors," MRS Online Proc. Library Arch. **1807**, 1–6 (2015).

[11]S. Frasca, B. Korzh, M. Colangelo, D. Zhu, A. Lita, J. Allmaras, E. Wollman, V. Verma, A. Dane, E. Ramirez, A. Beyer, S. Nam, A. Kozorezov, M. Shaw, and K. Berggren, "Determining the depairing current in superconducting nanowire single-photon detectors," Phys. Rev. B **100**, 054520 (2019).

[12]C. Zhang, W. Zhang, J. Huang, L. You, H. Li, C. Lv, T. Sugihara, M. Watanabe, H. Zhou, Z. Wang, and X. Xie, "NbN superconducting nanowire single-photon detector with an active area of 300 $\mu$m-in-diameter," AIP Adv. **9**, 075214 (2019).

[13]S. M. George, "Atomic layer deposition: An overview," Chem. Rev. **110**, 111–131 (2010).

[14]D. R. Boris, V. D. Wheeler, N. Nepal, S. B. Qadri, S. G. Walton, and C. C. R. Eddy, "The role of plasma in plasma-enhanced atomic layer deposition of crystalline films," J. Vacuum Sci. Technol. A **38**, 040801 (2020).

[15]N. E. Richey, C. de Paula, and S. F. Bent, "Understanding chemical and physical mechanisms in atomic layer deposition," J. Chem. Phys. **152**, 040902 (2020).

[16]H. Kim, "Characteristics and applications of plasma enhanced-atomic layer deposition," Thin Solid Films **519**, 6639–6644 (2011).

[17]M. Ukibe and G. Fujii, "Superconducting characteristics of NbN films deposited by atomic layer deposition," IEEE Trans. Appl. Supercond. **27**, 1–4 (2017).

[18]J. Musschoot, Q. Xie, D. Deduytsche, S. Van den Berghe, R. Van Meirhaeghe, and C. Detavernier, "Atomic layer deposition of titanium nitride from TDMAT precursor," Microelectron. Eng. **86**, 72–77 (2009).

[19]C. Sheagren, P. Barry, E. Shirokoff, and Q. Y. Tang, "Atomic layer deposition niobium nitride films for high-Q resonators," J. Low Temp. Phys. **199**, 875–882 (2020).

[20]P. Yagoubov, G. Gol'tsman, B. Voronov, L. Seidman, V. Siomash, S. Cherednichenko, and E. Gershenzon, "The bandwidth of HEB mixers employing ultrathin NbN films on sapphire substrate," in Proceedings of 7th International Symposium on Space Terahertz Technology (1996), p. 290.

[21]E. Knehr, A. Kuzmin, D. Y. Vodolazov, M. Ziegler, S. Doerner, K. Ilin, M. Siegel, R. Stolz, and H. Schmidt, "Nanowire single-photon detectors made of atomic layer-deposited niobium nitride," Supercond. Sci. Technol. **32**, 125007 (2019).

[22]R. Cheng, S. Wang, and H. X. Tang, "Superconducting nanowire single-photon detectors fabricated from atomic-layer-deposited NbN," Appl. Phys. Lett. **115**, 241101 (2019).

[23]A. J. Kerman, E. A. Dauler, W. E. Keicher, J. K. Yang, K. K. Berggren, G. Gol'tsman, and B. Voronov, "Kinetic-inductance-limited reset time of superconducting nanowire photon counters," Appl. Phys. Lett. **88**, 111116 (2006).

[24]L. A. Giannuzzi and F. A. Stevie, "A review of focused ion beam milling techniques for TEM specimen preparation," Micron **30**, 197–204 (1999).

[25]R. H. Hadfield, "Single-photon detectors for optical quantum information applications," Nat. Photonics **3**, 696–705 (2009).

[26]J. R. Clem and K. K. Berggren, "Geometry-dependent critical currents in superconducting nanocircuits," Phys. Rev. B **84**, 174510 (2011).

[27]A. Kozorezov, C. Lambert, F. Marsili, M. Stevens, V. Verma, J. Allmaras, M. Shaw, R. Mirin, and S. W. Nam, "Fano fluctuations in superconducting-nanowire single-photon detectors," Phys. Rev. B **96**, 054507 (2017).

[28]F. Marsili, F. Najafi, E. Dauler, F. Bellei, X. Hu, M. Csete, R. J. Molnar, and K. K. Berggren, "Single-photon detectors based on ultranarrow superconducting nanowires," Nano Lett. **11**, 2048–2053 (2011).

[29]H. Zhou, Y. He, L. You, S. Chen, W. Zhang, J. Wu, Z. Wang, and X. Xie, "Few-photon imaging at 1550 nm using a low-timing-jitter superconducting nanowire single-photon detector," Opt. Express **23**, 14603–14611 (2015).

[30]S. D. Dyer, M. G. Tanner, B. Baek, R. H. Hadfield, and S. W. Nam, "Analysis of a distributed fiber-optic temperature sensor using single-photon detectors," Opt. Express **20**, 3456–3466 (2012).

[31]H. Takesue, S. W. Nam, Q. Zhang, R. H. Hadfield, T. Honjo, K. Tamaki, and Y. Yamamoto, "Quantum key distribution over a 40-dB channel loss using superconducting single-photon detectors," Nat. Photonics **1**, 343–348 (2007).

[32]A. Biswas, M. Srinivasan, S. Piazzolla, and D. Hoppe, "Deep space optical communications," Proc. SPIE **10524**, 105240U (2018).

[33]K. M. Rosfjord, J. K. Yang, E. A. Dauler, A. J. Kerman, V. Anant, B. M. Voronov, G. N. Gol'tsman, and K. K. Berggren, "Nanowire single-photon detector with an integrated optical cavity and anti-reflection coating," Opt. Express **14**, 527–534 (2006).

[34]K. Erotokritou, R. M. Heath, G. G. Taylor, C. Tian, A. Banerjee, A. Casaburi, C. M. Natarajan, S. Miki, H. Terai, and R. H. Hadfield, "Nano-optical photoresponse mapping of superconducting nanowires with enhanced near infrared absorption," Supercond. Sci. Technol. **31**, 125012 (2018).

[35]N. Calandri, Q.-Y. Zhao, D. Zhu, A. Dane, and K. K. Berggren, "Superconducting nanowire detector jitter limited by detector geometry," Appl. Phys. Lett. **109**, 152601 (2016).

[36]A. Banerjee, R. M. Heath, D. Morozov, D. Hemakumara, U. Nasti, I. Thayne, and R. H. Hadfield, "Optical properties of refractory metal based thin films," Opt. Mater. Express **8**, 2072–2088 (2018).

[37]S. Steinhauer, S. Gyger, and V. Zwiller, "Progress on large-scale superconducting nanowire single-photon detectors," Appl. Phys. Lett. **118**, 100501 (2021).